

Fermi Surface of Lithium by Positron Annihilation*

J. J. DONAGHY† AND A. T. STEWART

University of North Carolina, Chapel Hill, North Carolina

(Received 15 May 1967)

The angular correlation of radiation from positrons annihilating in lithium single crystals has been measured. The crystals were oriented in the [100], [110], and [111] directions, and the measurements yield information closely related to the areas of slices through the Fermi surface normal to these directions. The measurements show that the Fermi surface of lithium is anisotropic, the length of the radius vector k_{110} being about 5% greater than k_{100} . The measurements also yield estimates of the energy gap at the boundary of the first Brillouin zone, and the amplitudes of the most important higher-momentum components of the electron wave function.

I. INTRODUCTION

FOR a number of years, the angular correlation of annihilation radiation has been used to obtain information about the shape of the Fermi surface.¹ Early measurements made on beryllium^{2,3} and magnetium³ indicated the possibility of obtaining anisotropies in the photon momentum distribution in experiments with oriented single crystals, and such anisotropies can be related to departures from sphericity in the shape of the Fermi surface. Indeed more recent experiments and calculations on the electron structure of holmium⁴ and yttrium⁵ have shown the value of positron-annihilation data for testing band-structure calculations. This paper describes a series of similar experiments on single crystals of lithium. These measurements provide quantitative estimates of the radii to the Fermi surface in the [100], [110], and [111] directions. In addition, they provide estimates of the energy gap at the boundary of the first Brillouin zone and the amplitudes of the higher-momentum components of the Bloch wave function. A preliminary account of this work has already been given.⁶

II. PHOTON MOMENTUM DISTRIBUTION

The technique of using positron annihilation to obtain the momentum distribution of electrons has

* Research supported by the National Science Foundation.

† Present address: Physics Department, Washington and Lee University, Lexington, Virginia.

¹ A review of the subject is given by A. T. Stewart, in *Positron Annihilation*, edited by A. T. Stewart and L. O. Roellig (Academic Press Inc., New York, 1967) and by P. R. Wallace, in *Solid State Physics*, edited by F. Seitz and D. Turnbull (Academic Press Inc., New York, 1960), Vol. 10 p. 1.

² A. T. Stewart, J. B. Shand, J. J. Donaghy, and J. H. Kusmiss, *Phys. Rev.* **128**, 118 (1962).

³ S. Berko, *Phys. Rev.* **128**, 2166 (1962).

⁴ R. W. Williams, T. L. Loucks, and A. R. Mackintosh, *Phys. Rev. Letters* **16**, 168 (1966).

⁵ T. L. Loucks, *Phys. Rev.* **144**, 504 (1966).

⁶ This work formed part of the Ph.D. thesis of one author (J.J.D., University of North Carolina, 1964) and has been published in abbreviated form in: A. T. Stewart, J. J. Donaghy, J. H. Kusmiss, and D. M. Rockmore, *Bull. Am. Phys. Soc.* **9**, 238 (1964); J. J. Donaghy, A. T. Stewart, D. M. Rockmore, and J. H. Kusmiss, in *Low Temperature Physics, LT9*, edited by J. G. Daunt, D. O. Edwards, F. J. Milford, and M. Yaquub (Plenum Press Inc., New York, 1965), p. 835. A more detailed theoretical paper comparing calculations with these data has been published by DeBenedetti and Melngailis (Ref. 15) in 1966.

often been described.¹ In brief, if the annihilating electron is in the state ψ_k , the probability that a pair of photons will be emitted with momentum $\mathbf{p}=\hbar\mathbf{K}$ is proportional to⁷

$$\rho_k(\mathbf{K}) = \left| \int_{\text{crystal}} \psi_k(\mathbf{r})\psi_+(\mathbf{r}) \exp(-i\mathbf{K}\cdot\mathbf{r}) d\mathbf{r} \right|^2, \quad (1)$$

where ψ_+ is the positron wave function. The momentum distribution of the photon pairs is then proportional to

$$\rho(\mathbf{K}) = \sum_{\mathbf{k}} \rho_{\mathbf{k}}, \quad (2)$$

the summation extending over all occupied states in k space. The counting rate measured by the long-slit apparatus is proportional to

$$N(\theta) = \int \rho(K) dK_x dK_y, \quad (3)$$

where $\theta=\hbar K_z/mc$ is the amount by which the angle between the two photons differs from 180° . The instrument resolution was: detector slit width/source-detector distance=0.050 in./250 in.= 0.2×10^{-3} rad.

III. EXPERIMENTAL RESULTS

The data obtained in this series of experiments are shown in Fig. 1. Corrections have been made for the decay of the positron source, and the areas under the curves drawn through the points have been normalized to the same total number or counts. Otherwise, the data are shown exactly as they were obtained in the experiments. The curves through the experimental points will henceforth be called "angular-correlation curves" or simply "curves."

The central, roughly parabolic portion of each curve arises mainly from annihilations with conduction electrons. These "parabolas" have a fairly sharp cut off at the angle θ_f , defined by the equation $m c \theta_f = \hbar k_f$, k_f being the radius of the free-electron sphere. The broad, bell-shaped part of each curve arises primarily from annihilation with core electrons. There is also a small contribution to this part of the distribution from the higher-momentum components (HMC) of the con-

⁷ S. DeBenedetti *et al.*; *Phys. Rev.* **77**, 205 (1950).

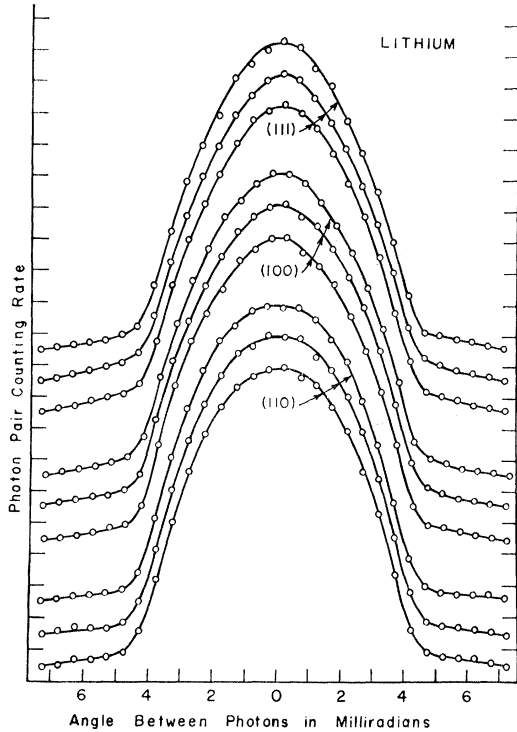


FIG. 1. The angular-correlation curves for the three principal directions of lithium. The angle between the photons is related to the photon momentum by the equation $p_z/mc = \theta$.

duction-electron wave function. The contribution of the HMC is different for the three directions. For values of $\theta > \theta_f$, the contribution of the HMC is small, but significant.

It is convenient to subtract out the part of the distribution due to core electrons. This was done by fitting a Gaussian-type curve to the measured [100] distribution in the range of 5–6 mrad. The same curve was then subtracted from the measurements for all three directions, thus preserving any differences in the three distributions. The data after subtraction are shown in Fig. 2.

Two important conclusions can be reached at once without detailed analysis:

(a) The Fermi surface of lithium is anisotropic. The differences between the curves for the three directions are appreciably greater than the experimental error of about 1%.

(b) The Fermi surface does not touch the zone boundary in the [110] direction unless it does so by an unrealistically narrow neck. The cut off in the [110] direction is at approximately $\theta = 4.33$ mrad, whereas the boundary of the first zone is at $\theta = 4.95$ mrad.

IV. ANALYSIS OF DATA

The parameters of interest in specifying the shape of the Fermi surface are the radii in the principal

directions. Estimates of these radii have been obtained in the following manner:

First of all, a phenomenological model of the Fermi surface containing several adjustable parameters was chosen. The areas of slices through this model normal to the three principal directions were then calculated. If each annihilation with a conduction electron resulted in a photon pair with momentum $\mathbf{p} = \hbar\mathbf{k}$, the crystal momentum of the electron, then the measured distribution would be directly proportional to the areas of such slices. Since some annihilations result in photon pairs with momentum $\hbar(\mathbf{k} - \mathbf{G})$, \mathbf{G} being a reciprocal lattice vector, the measured distribution will not be proportional to these areas. However, if the amplitudes of the higher-momentum components are small—which an inspection of the measurements indicates is true—their effect can be treated as a small correction to the calculated areas. This is the procedure followed in analyzing the results of this experiment.

The model chosen to fit the data consists of a sphere of radius r with 12 bumps superimposed toward the zone boundaries. If a given point on the sphere is labeled with the spherical coordinates (r, θ, ϕ) (the θ here should not be confused with the correlation angle θ), and the distance from this point to the nearest zone boundary is denoted by $d(\theta, \phi)$, then the radius to the Fermi surface in this direction is given by the model as

$$k_F(\theta, \phi) = r + \Delta r = r + A \exp[-\alpha d(\theta, \phi)]. \quad (4)$$

The model contains the adjustable parameters r , A , and α , their values being fixed by choosing values of k_F in the [100], [110], and [111] directions consistent with the requirement that the enclosed volume equal the volume of the free-electron sphere. After fixing the shape of the model, the areas of slices at 50 equally spaced points along the radius vector in each of the three principal directions were calculated.⁸ Calculations were made for a series of values of the three principal radii: k_{100} , k_{110} , and k_{111} . In Fig. 3 is shown the result of a calculation using the values $k_{110} = 1.04 k_f$, $k_{111} = k_{100} = 0.99 k_f$. It can be seen that the calculated areas have the same form as the measured distribution in the range $0 < \theta < 2.5$ mrad. The difference in the calculated areas and the measurements for $\theta > 2.5$ mrad can be attributed to the HMC.

Effect of HMC

In a series of recent papers,⁹ several authors have shown that a good single particle approximation for

⁸ We are much indebted to Dr. D. M. Rockmore for this calculation.

⁹ C. Herring, Phys. Rev. 57, 1169 (1940); M. H. Cohen and V. Heine, Advan. Phys. 1, 395 (1958); J. C. Phillips and L. Kleinman, Phys. Rev. 116, 287 (1959).

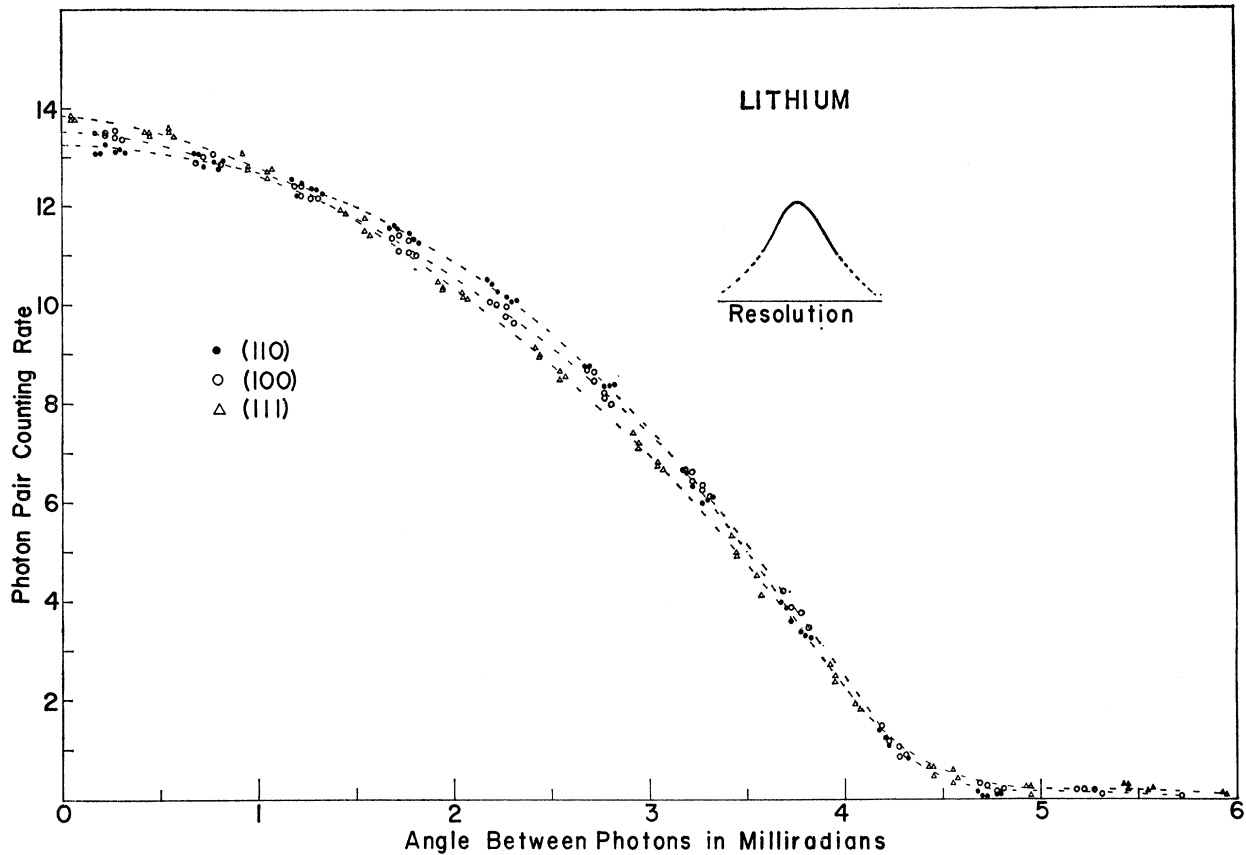


FIG. 2. The angular-correlation curves for lithium after subtraction of the background due to annihilations with core electrons, and folding about 0° . The dashed lines through the points represent a visual fit to the data.

the wave function for a conduction electron has the form

$$\psi_{\mathbf{k}} = \phi_{\mathbf{k}} - \sum_{\mathbf{c}} (\phi_{\mathbf{k}}, \phi_{\mathbf{c}}) \phi_{\mathbf{c}}. \quad (5)$$

In this expression $\phi_{\mathbf{k}}$, the so-called "smooth part" of the wave function has the form

$$\phi_{\mathbf{k}} = \sum_{\mathbf{G}} a_{\mathbf{G}}(\mathbf{k}) \exp[i(\mathbf{k} - \mathbf{G}) \cdot \mathbf{r}]. \quad (6)$$

In general the sum extends over several vectors of the reciprocal lattice. The second term in (5) is a linear combination of core states, $\phi_{\mathbf{c}}$, and accurately describes the rapid oscillations of $\psi_{\mathbf{k}}$ inside the core. Since the positron is effectively excluded from the core by the Coulomb repulsion¹⁰ it will "sample" only the smooth part of $\psi_{\mathbf{k}}$. Outside the core the amplitude of $\psi_{\mathbf{k}}$ is approximately constant. The photon momentum distribution can thus be written approximately as

$$\rho(\mathbf{K}) = \sum_{\mathbf{k}} \left| \int_{\text{crystal}} \phi_{\mathbf{k}} \exp(-i\mathbf{K} \cdot \mathbf{r}) d^3\mathbf{r} \right|^2. \quad (7)$$

the summation extending over all occupied states in

¹⁰ See, for example, calculations of S. Berko and J. S. Plaskett, Phys. Rev. **112**, 1877 (1958).

k space. The distribution of the z component of \mathbf{K} becomes, after inserting the expression (6) for $\phi_{\mathbf{k}}$,

$$N(K_z) \propto \sum_{\mathbf{G}} \int |a_{\mathbf{G}}(\mathbf{K} + \mathbf{G})|^2 dK_x dK_y, \quad (8)$$

if $\mathbf{K} + \mathbf{G}$ lies inside the Fermi surface. For other values of $\mathbf{K} + \mathbf{G}$, $N(K_z) = 0$.

If $\phi_{\mathbf{k}}$ contained only one term, $a_0 \exp(-i\mathbf{k} \cdot \mathbf{r})$, the Fermi surface would be spherical and $N(K_z)$ would have the form

$$\begin{aligned} N(K_z) &\propto 1 - K_z^2/k_f^2, & 0 < K_z < k_f \\ &\propto 0, & K_z > k_f \end{aligned} \quad (9)$$

which is a parabola. This is the form of the measured distribution for sodium.¹¹ Since the data of Fig. 2 indicate that the Fermi surface of lithium is only slightly distorted, it will be assumed that $\phi_{\mathbf{k}}$ can be written in

¹¹ Because the annihilation probability is slightly velocity-dependent, the angular-correlation curves for sodium are not quite parabolic. This effect is also present in lithium, but does not affect the statements made in this paper. This velocity dependence is discussed in the following paper. A short discussion may be found in Ref. 6.

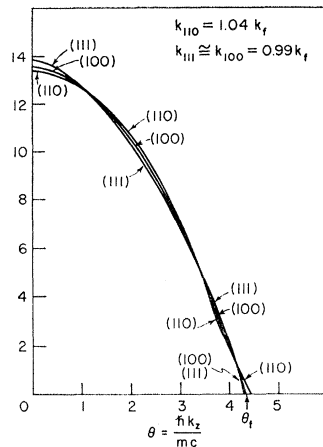


FIG. 3. The areas of cross sections through the Fermi surface normal to the three principal directions as calculated from the model discussed in the text. The model parameters were fixed by setting the calculated areas at 0° equal to the measured counting rates. The calculated areas at 0° correspond to extremal areas through the Fermi surface as obtained in this experiment.

the almost-free-electron approximation as

$$\phi_{\mathbf{k}} = a_0 \exp(i\mathbf{k} \cdot \mathbf{r}) + a_G \exp[i(\mathbf{k} - \mathbf{G}) \cdot \mathbf{r}], \quad (10)$$

\mathbf{G} being the reciprocal lattice vector normal to the zone boundary nearest the point \mathbf{k} . If an electron in the state \mathbf{k} annihilates, the resulting photon pair will have momentum $\hbar\mathbf{k}$ or $\hbar(\mathbf{k} - \mathbf{G})$, with relative probabilities $|a_0|^2$ and $|a_G|^2$.

The amplitude a_G was calculated from the equation¹²

$$a_G = (2mV/\hbar^2)[a_0/K^2 - (\mathbf{K} - \mathbf{G})^2] \quad (11)$$

for an energy gap $V=3\text{eV}$. (See for example Refs. 13 and 14.) Table I gives several values of a_G obtained in this manner, assuming that $|a_0|^2 + |a_G|^2 = 1$. Although the value of a_G is quite large near the Fermi radius k_f , its value diminishes rapidly as the distance from the zone boundary increases. Therefore, only a few states near the zone boundary will contain an appreciable higher-momentum component. For this reason, most of the annihilations are normal processes, and only a few percent of the photons arise from umklapp annihilations and have momentum $\hbar(\mathbf{k} + \mathbf{G})$.

TABLE I. Amplitude of HMC.

k_z/k_f	$ a_G ^2$
1.0	0.140
0.9	0.065
0.8	0.035
0.7	0.025

¹² N. F. Mott and H. Jones, *The Theory of the Properties of Metals and Alloys* (Oxford University Press, New York, 1936).

¹³ F. S. Ham, *Phys. Rev.* **128**, 82 (1962).

¹⁴ F. S. Ham, *Phys. Rev.* **128**, 2524 (1962).

An approximate calculation has been made of the quantity

$$\int_{\text{occupied states}} |a_G(\mathbf{k})|^2 d\mathbf{k}_x d\mathbf{k}_y.$$

This quantity, or some integral multiple of it, must be added to the calculated areas for some values of θ , and subtracted at other values. Since the geometry becomes rather involved, only the results will be given here. These results are shown in Fig. 4, in which the loss in counting rate due to the HMC is plotted versus θ . It can be seen from this graph that, roughly speaking the effect of the HMC for the $[100]$ and $[111]$ directions is to decrease the measured counting rate in the range 2–4 mrad and to increase the counting rate in the range 4–6 mrad. For the $[110]$ direction, the

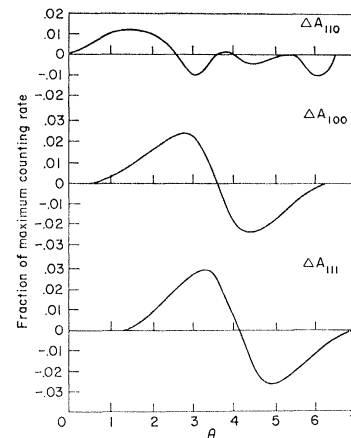


FIG. 4. The amount ΔA shown above must be subtracted from the calculated areas of Fig. 3 for comparison with the measured counting rates.

effect of the HMC is to decrease the counting rate in the range 1–3 mrad. However, the decrease should be only about 1% of the maximum counting rate, which is approximately the same as the experimental error of the measurements. Therefore, the effect of the HMC on the $[110]$ measurements can be considered negligible. The HMC should also produce a small bump in the $[110]$ angular correlation curve at about 6 mrad. Again however, the expected increase is within the experimental error.

One circumstance makes it possible to determine the model parameters independently of a consideration of the effects of the HMC or of the enhancement effect discussed in a succeeding paper. In the neighborhood of $K_z=0$, the photon pairs with momentum $\hbar\mathbf{k}$ and $\hbar(\mathbf{k} - \mathbf{G})$ have the same z component of momentum. For this reason, the HMC produce no net effect near 0° . The measured distribution at this point, therefore, should be directly proportional to the extremal areas

of slices through the Fermi surface. The model parameters can thus be chosen so that these areas "fit" the measured results at 0° . The measured counting rates at 0° can be compared directly with Ham's calculation of the extremal areas for the three principal directions. Ham obtained the values^{13,14}

$$\begin{aligned}(A_{111} - A_{110})/A_{110} &\simeq 0.036, \\ (A_{100} - A_{110})/A_{110} &\simeq 0.017.\end{aligned}$$

These values compare favorably with our results of 0.045 ± 0.012 and 0.020 ± 0.012 , respectively. For the values of the principal radii Ham obtains

$$k_{110} = 1.023k_f, \quad k_{100} = 0.973k_f, \quad k_{111} = 0.983k_f,$$

whereas we obtain

$$k_{110} = 1.04k_f, \quad k_{111} \simeq k_{100} = 0.99k_f.$$

Therefore, using our model we obtain somewhat sharper bumps than Ham predicts.

The shape of a slice through the bump in the [110] direction, as obtained from the model with the principal radii listed above, is shown in Fig. 5. The ratio k_F/k_f is plotted as a function of the angular distance from the [110] direction. The variation of k_F in two separate planes is shown. In the interval from the origin (45°) to zero, k_F lies in the plane containing the [110] and [100] directions. In the interval from 0° to 90° , k_F lies in the plane containing the [110], [111], and [001] directions. From this graph it is easy to visualize the shape of the Fermi surface of lithium as obtained by this analysis of these experiments.

Possibility of Direct Observation of HMC

The results shown in Fig. 4 indicate that the contribution of the HMC to the counting rate for the

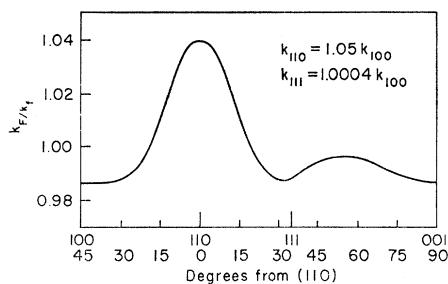


FIG. 5. The radius of the Fermi surface in various directions as computed from our phenomenological model. The estimated accuracy is about $1\frac{1}{2}\%$ in k_F .

[111] measurements should reach a maximum at $\simeq 5$ mrad, which is appreciably greater than θ_f , (4.33 mrad), and also outside the portion of the angular correlation curve most strongly affected by the finite angular resolution of the experiment. A careful study of Fig. 1 indicates that the measured counting rate for the [111] direction is consistently higher than for the other two directions, which lends support to the arguments given above. The "statistics" for measurements in this region are poor, however, so that many more measurements should be made before a direct measurement of the effects of the HMC can be said to have been made. The measurements also indicate a slight bump near 6 mrad for the [110] curve, but again the effect is of about the same size as the statistical error.

V. CONCLUSIONS

The principal conclusions derived from this experiment are as follows:

- (1) The Fermi surface of lithium is anisotropic, k_{110} being about 5% greater than k_{100} .
- (2) The Fermi surface does not touch zone boundary in the [110] direction, unless it does so by a very thin "neck".
- (3) The Fermi surface and energy bands calculated by Ham are in agreement with these results which are estimated to be accurate to about $1\frac{1}{2}\%$ in k_f .

Some of the assumptions made in analyzing the results of this experiment can be verified only by complete calculations of ψ_k , ψ_+ , and the energy as a function of \mathbf{k} . Such a calculation has been made by Melngailis,¹⁵ who calculated the band structure and the positron-annihilation results by a pseudopotential technique. He not only calculated the twelve nearest [110] orthogonalized-plane-wave (OPW) coefficients more accurately than were done here but in addition the next six [200] OPW terms and the positron wave functions. It is satisfying that his work is in substantial agreement with our simpler, more approximate, calculations and especially pleasing that both calculations fit the data reasonably well.

ACKNOWLEDGMENTS

We are happy to acknowledge the assistance of colleagues Dr. J. H. Kusmiss and Dr. J. B. Shand and especially the extensive calculations of Dr. D. M. Rockmore.

¹⁵ J. Melngailis and S. DeBenedetti, Phys. Rev. **145**, 400 (1966).